

©2017, Elsevier. Licensed under the Creative Commons Attribution-NonCommercial-NoDerivatives 4.0 International <http://creativecommons.org/about/downloads>



Comparison of the behaviour of steel, pure FRP and hybrid shear walls under seismic loading in aspect of stiffness degradation and energy absorption

Natalja Petkune^{1*}, Ted Donchev^{2*}, Homayoun Hadavinia³, David Wertheim⁴,
Mukesh Limbachiya²

¹ CampbellReith, Raven House, 29 Linkfield Lane, Redhill, RH1 1SS, UK.

² Department of Civil Engineering, Kingston University London, KT1 2EE, UK.

³ Department of Mechanical & Automotive Engineering, Kingston University London, SW15 3DW, UK.

⁴ Department of Computer Science, Kingston University London, KT1 2EE, UK.

Abstract

Introducing of light-weight lateral load resisting systems, such as steel shear walls (SSW) is very beneficial for multi-storey buildings. Further improvement of such elements via introducing fibre reinforced polymer (FRP) materials is expected to allow increasing of their ultimate load capacity, stiffness and energy absorption. The aim of presented research is to compare the behaviour of modified SSW via inclusion of FRP in infill plate design. Produced and tested samples are three different types: with steel infill plate (control), with FRP infillplate and with hybrid steel/FRP infill plate. All samples are loaded under quasi-static cyclic seismic testing load as defined in ATC 24 protocol (ATC 24, 1992). The highest ultimate load capacity and lowest stiffness degradation is achieved for sample with glass FRP infill plate, followed by hybrid (carbon FRP/steel and glass FRP/steel) samples. Highest cumulative energy absorption for predominant part of the investigated amplitudes was achieved for hybrid samples. The obtained results indicate that the innovative shear walls with FRP and hybrid infill plates offer excellent load capacity and energy absorption, relatively small loss of stiffness and potential for increased durability in comparison with conventional SSW systems.

Keywords: Shear walls; Hybrid plates; Stiffness degradation; Energy absorption; Seismic loading, FRP

1. INTRODUCTION

Steel shear walls (SSWs) have become popular lateral resisting system in the last three decades. SSW consists of horizontal and vertical boundary elements bounding a thin steel infill plate inside. The resulting system is a stiff cantilever which acts as a vertical plate girder where columns can be treated as flanges and steel plate as web. Advantages of SSW system such as substantially large displacement ductility, high initial stiffness, large energy absorption capacity, fast pace of

* Corresponding authors: Email: NataljaPetkune@campbellreith.com (Natalja Petkune); T.Donchev@kingston.ac.uk (Ted Donchev).

construction, small wall thickness and small seismic mass have made them preferable in seismic design in many cases in comparison to other lateral load resisting systems [1], [2], [3].

SSWs are often used in earthquake resistant design for tall structures in Japan and North America. The first building incorporating the SSW system is the Shin Nittetsu Building in Tokyo, Japan completed in 1970. Five continuous H-shaped shear walls were built for 20-storey office tower [4]. The first important building with SSWs, which experienced two significant earthquakes and damages occurred only to non-structural elements, was built in USA is Sylmar Hospital in Los Angeles [1].

Fibre reinforced polymers (FRP) are often used as a strengthening material for structures which undergo substantial damages or require additional capacity due to change of design brief [5], [6]. Structural elements with carbon FRP (CFRP) and glass FRP (GFRP) are becoming popular in thin walled structures, sandwich panels and shear walls due to the combination of benefits from different materials. Initial research about FRP repair and straightening of damaged SSW and hybrid SW indicates opportunities for fast and effective recovery of the capacity of the damaged shear walls of this type [7].

The aim of this research is to investigate the performance of the shear wall system via inclusion of pure FRP as well as a combination of steel and FRP as one of the main structural components for the infill plates of the innovative shear walls. In total three types of infill plates for shear wall were investigated – one type of infill plates was hybrid of steel and FRP, the other was made of pure FRP and infill plate for control specimen was made from steel. The shear wall specimens were tested under cyclic sinusoidal loading with horizontal displacement loading increasing from 0.2 mm up to 30 mm in accordance with the ATC-24 protocol [8]. The results of ultimate load capacity and energy absorption within the testing interval for different shear wall systems were measured and compared. The degradation of stiffness values at peak load of each cycle for all specimens and dynamic stiffness of all specimens through entire loading were estimated and the results were analysed.

2. BACKGROUND

2.1 Steel Shear walls

The effectiveness of the steel shear wall for seismic design under laboratory conditions were investigated by many researchers in the United States, Japan, Canada and the United Kingdom. The first analytical models were developed by Thorburn et al. [9] who investigating the effects of varying the thickness of infill plate and the angle of the inclination of the tension field for different height/width ratio on post-buckling capacity.

Stiffened and unstiffened steel shear walls have been introduced in many buildings around the world. In some cases heavy stiffeners are used in order to increase the buckling capacity of shear

wall and to obtain high energy absorption during post-buckling [10], [11]. In order to achieve higher stiffness and deformability of shear wall system, steel infill plates can be reinforced by addition of concrete layer using shear studs on one or both sides of the steel plate [12], [13]. Other way for improving SSW performance is using hybrid shear wall by bonding FRP laminate to the steel infill plate.

2.2 Hybrid steel/FRP shear walls

Hybrid shear walls (HSW) are defined as steel boundary elements with infill plate either laminated with FRP material or made completely from FRP material. HSWs are innovative structural lateral load resisting system and have significant advantages in comparison with steel shear wall systems. These include increased in-plane stiffness and load carrying capacity of the system and more uniform distribution of the tension field resulting in reduction of out-of-plane deformations in the infill plate [14, 7].

Maleki et al. [15] conducted experimental and numerical studies investigating behaviour of the medium scale hybrid steel/GFRP shear walls with and without openings. They concluded that when steel plate is laminated with GFRP material, during quasi-static testing following the ATC-24 protocol more uniform distribution of the tension field within infill plate is observed and out-of-plane deformations are reduced significantly. Application of GFRP material significantly improved the stiffness and the strength of the system in comparison with a control consisting of a steel shear wall. Similar conclusions were made by Nateghi-Alahi and Khazaei- Pul [16] when testing hybrid steel/GFRP specimens under fully reversed cyclic quasi-static loading. Hybrid specimens achieve higher ultimate strength and increase the cumulative energy dissipation.

For design optimisation, numerical studies investigating the one-storey hybrid steel/CFRP shear wall with different fibres orientation and lay-ups were carried out by Rahai and Alipour [17]. It was found that the optimum CFRP fibres orientation is the angle of inclination of the tension field in the infill plate. When this angle is applied, significant increases in strength and stiffness were noticed. It was also noted that application of the FRP does not change dramatically the stress distribution within the infill plate at initial stages of testing; however when the plate has yielded, FRP composites layer carries significant loads in the direction of the tension field. Hatami et al. [18] carried out experimental and numerical studies and developed equations and graphs regarding the influence of different inclination of CFRP fibres on shear capacity, ductility, energy dissipation and stiffness ratios.

Comparison between two types of steel/GFRP and steel/CFRP hybrid specimens were investigated by Petkune et al. [19]. Similar behaviour of the specimens was recorded when significant failure in the connection between fish plates and the infill plate occurred. Investigation of hybrid

connections showed that the addition of an adhesive bonding significantly improved the connection's capacity. Another important damage mechanism for these specimens was the delamination of the FRP layers and debonding from the steel of the infill plate. The delaminations and debonding were monitored using the infrared thermography (IRT) following external heating of one side of the infill plate at the end of the loading cycles [20], [21].

3. METHODOLOGY

3.1 Description of the specimens

The experimental protocol included testing of five single-storey medium scale shear wall specimens. These specimens consist of steel frames with the same dimensions for all specimens (Figure 1) and infill plates with different design specifications depending on the type of the specimens. The steel frames were made from steel (grade S355), fabricated and assembled from Universal Beam Section 127x76x13 mm. The frames were designed at Kingston University London, and then assembled and produced (Cannon Steels Ltd, Enfield, Middlesex, UK). Primary fish plates were welded to the steel frame.

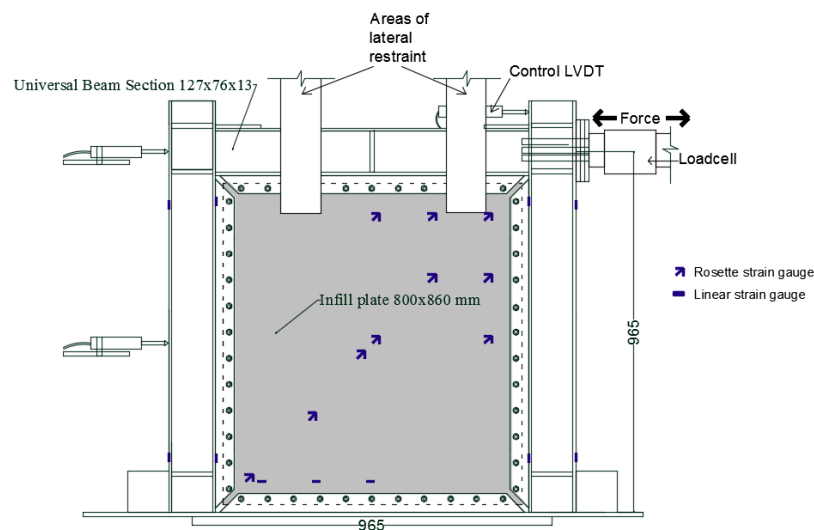


Figure 1. Dimensions of single-storey steel shear wall and scheme for loading equipment.

Five tested specimens are differentiated by infill plates: control steel shear wall (SSW), pure CFRP shear wall (CSW), pure GFRP shear wall (GSW), hybrid CFRP/steel shear walls (HCSW) and hybrid GFRP/steel shear wall (HGSW).

The control SSW specimen was made from a steel frame of S355 grade and the steel infill plate with the thickness of 0.8 mm was made from S275 steel grade.

Group 1 pure FRP specimens (CSW and GSW) were made from eight layers of unidirectional (UD) CFRP or GFRP plies laminated on steel infill plates within steel boundary elements. For the CSW specimen, CFRP prepreg type MTM 28-1 series was supplied by Cytec Industrial Material Ltd (Derby, UK) and for GSW specimen GFRP prepreg with epoxy resin E722-02 was supplied by Tencate

Advanced Composites Ltd (Nottingham, UK). The materials properties of prepreg CFRP and GFRP fabrics are shown in Table 2. For preparation of specimens, eight layers of the prepreg FRP were laid between steel cover plates at $\pm 45^\circ$ inclination angle of fibres relative to the loading direction in accordance with the details shown in Table 1.

Table 1. Specification of tested shear wall system specimens.

Group	Name of the specimen	Lay-up of infill plate	Weight of the infill plate, kg	Thicknesses of the infill plate, mm
Steel specimen	Steel Shear Wall (SSW)	[S]	4.08	0.80
Group 1: pure FRP specimens	Carbon FRP Shear Wall (CSW)	[± 45] _{2s}	2.24	1.68
	Glass FRP Shear Wall (GSW)		3.26	2.52
Group 2: hybrid specimens	Bonded Hybrid Carbon FRP Shear Wall (HCSW)	[+45/-45/A/S/A/-45/+45]	5.53	1.70
	Bonded Hybrid Glass FRP Shear Wall (HGSW)		5.95	2.40

Note: S - 0.8 mm steel plate, A - EF72 adhesive film

Specimens were then vacuum bagged and cured in an oven following the manufacturer's curing cycle.

Group 2 hybrid specimens (HCSW and HGSW) are steel framed with hybrid infill plates. Infill plates of HCSW were prepared by laminating 0.8 mm thick steel infill plate with two layers of CFRP prepreg material on each side of the plate, whereas the HGSW was laminated with two layers of UD GFRP prepreg material. The same type of the CFRP and GFRP materials were used for hybrid specimens as for pure FRP specimens. For hybrid specimens, an additional EF72 adhesive film (manufactured by TenCate Advanced Composites Ltd, Nottingham, UK) with area weight of 100 g/m² was placed between the steel plate and FRP fabric to create a better bond between these surfaces. Epoxy film and FRP plies were laid on both sides of the steel infill plate, then the laminated plate was placed between two steel cover plates covered with non-stick PTFE film. The bagging and curing process was followed as for pure FRP specimens.

Table 2: Properties of the CFRP and GFRP materials.

	Young's Modulus E ₁₁ , GPa	Young's Modulus E ₂₂ , GPa	Shear Modulus G ₁₂ , GPa	Poisson's ratio, ν ₁₂
CFRP prepreg MTM 28-1	140	8.5	5.8	0.319
Unidirectional GFRP	41	10.5	3.3	0.311

3.2 Connection between infill plates and fish plates

Schemes for connecting the infill plate and fish plates of the steel frame are shown in Table 3. Three types of the connections (A, B and C) were used. All specimens have bolted connections between infill plates and primary fish plates. Hexagon M8 bolts were spaced at 70 mm distance centre to centre.

Type A connection was used for the SSW specimen by means of a bolted connection between infill plate and fish plates. Primary and secondary fish plates and infill plate edges were cleaned and roughened with sand paper and connected with bolts.

Table 3. Connection between primary and secondary fish plates in different specimens.

Specimens	Connection	Scheme for connections between infill plate and fish plate
SSW	Type A: bolted connection	<p>Primary fish plate M8 bolt Secondary fish plate Steel infill plate</p>
CSW & GSW	Type B: bolted and adhesive + additional steel strips	<p>Primary fish plate M8 bolt Secondary fish plate Epoxy plus adhesiv Composite infill plate Additional steel strips</p>
HCSW & HGSW	Type C: bolted and adhesive	<p>Primary fish plate M8 bolt Secondary fish plate Epoxy plus adhesiv Hybrid infill plate</p>

In order to provide stiff connection for CSW and GSW specimens with pure FRP infill plates, additional steel strips 30 mm wide and 1.5 mm thick were attached with adhesive on both sides around the edges of the plate to reduce the risk for local stress concentration and destruction of FRP. After curing of the adhesive, the holes for bolts were drilled. Then an infill plate with steel strips was attached to the fish plate with M8 bolts using adhesive connection Type B.

For hybrid HCSW and HGSW specimens, type C bolted connection between infill plate and fish plates was applied with a layer of two parts epoxy adhesive [22] having shear strength of 20 MPa. Before adhesive application, the steel and FRP surfaces were prepared by removing grease, dust and moisture. The FRP surface was abraded until the surface lost its gloss. The adhesive applied for the HCSW and HGSW specimens was cured at room temperature for 24 hours before testing.

3.3 Testing procedure

Specimens were tested under quasi-static displacement controlled loading in accordance with ATC-24 protocol [8]. Figure 2 shows cyclic sinusoidal loading applied from 0.2 mm to 35 mm displacement at a slow rate. The magnitude of the applying displacement was gradually increased from 0.05 mm/min at 0.2 mm displacement to 2.2 mm/min at 35 mm displacement. Initially, three cycles at each amplitudes were applied, and then from 15 mm displacement the number of cycles was decreased to two.

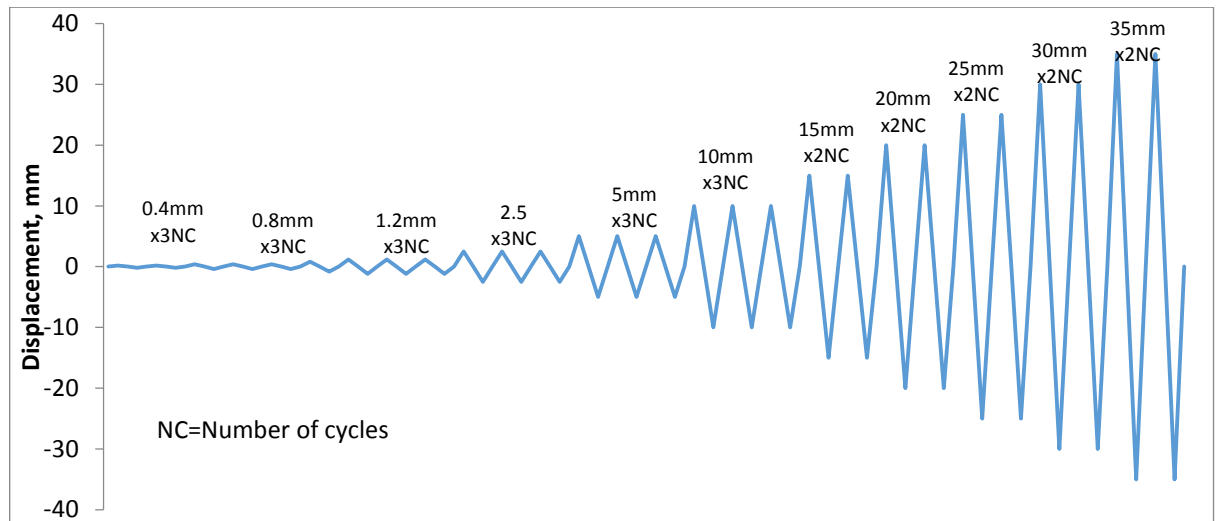


Figure 2. Quasi-static loading in accordance to ATC-24 protocol.

The testing rig consisted of a reaction frame and loading equipment. The base plate of the steel frame of specimens was bolted to the reaction frame and additional clamps were used to provide fully fixed positioning. The aim of lateral supports with rollers attached was to prevent early out-of-plane buckling of the shear wall specimen.

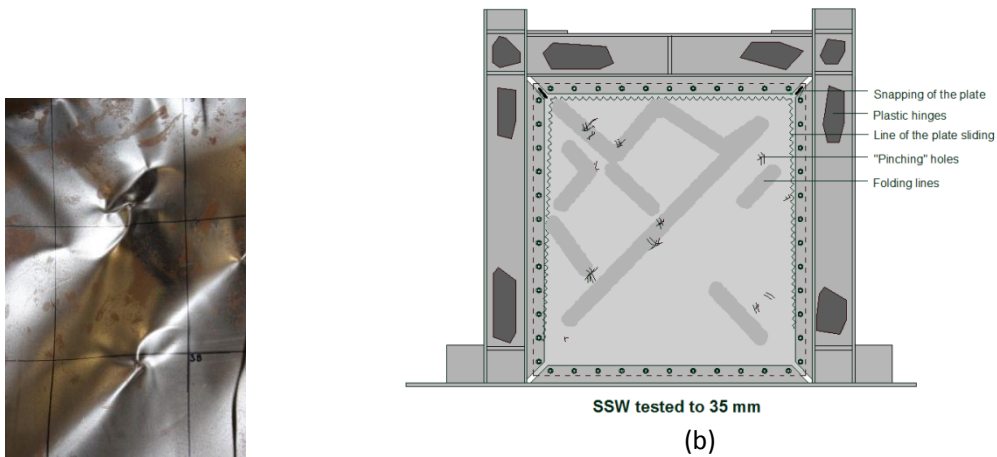
In plane horizontal displacement was applied via movement controlled by an inverter and screw jack. Several linear variable displacement transformers (LVDTs) and cable displacement sensors (CDS) were installed at different locations to measure displacements of the sample during testing. Measurements from LVDTs fixed to the loading plate, were used to control the displacement required for the completion of the loading cycle. The corresponding load applied to reach specific displacement was measured with a bi-directional load cell with a maximum capacity of 500 kN. All testing equipment was connected to a datataker, DT-85G, used record data. Delamination of the FRP material was monitored with the use of the IRT camera.

4. BEHAVIOUR OF SPECIMENS

4.1 Behaviour of SSW specimen

The first signs of developing plastic deformations appeared for displacements above 2.5 mm, when out-of-plate deformations were visible and initial shape was not recovering at the end of the

loading cycle. At a displacement greater than 10 mm, enlarging of holes around bolts in the connections between fish plates and infill plate started as well as a detection of sliding of the infill plate with respect to fish plates. Development of the plastic hinges was noticed at the bottom of the columns of steel frame at displacements higher than 15 mm. The initial pinching of the infill plate started at displacement of 15 mm, which further progressed to development of small “pinching” holes at displacements higher than 30 mm (Figure 3a) and development of plastic hinges at the top of the columns with 30 mm displacement. The final destruction of the steel shear wall specimen occurred through the development of the plastic hinges around the bottom and top areas of the column section and tearing of the steel plate around bolt holes close to the top parts of the frame (Figure 3b). The experiment was terminated at 35 mm displacement due to limitations of the testing equipment.



(a)

Figure 3. SSW a) appearance of “pinching” holes b) tested specimen at 35 mm displacements.

4.2 Behaviour of shear walls with FRP infill plate

4.2.1 CSW specimen

For the carbon fibre infill plate specimen (CSW) appearance of diagonal tension field was noticed at 2.5 mm displacement, which fully recovered up to a displacement of 5 mm.

Initial cracking of CFRP layers over part of the thickness of infill plate accompanied by delamination of teared layers at this area occurred for displacements higher than 5 mm. At the same time small cracks through the full thickness of the plate) started to appear in the corners of the infill plate. When displacements were increased to 15 mm, delamination of the CFRP perpendicular to the cracks was recorded. The layer of the adhesive of the connection between fish plates cracked when the specimen was tested to 20 mm displacement. Development of the plastic hinges was noticed at 20 mm displacement in the steel boundary elements. CSW achieved its ultimate load of 266 kN at 20

mm displacement. Testing was terminated at 25 mm displacement with significant cracks having developed in the direction of diagonal tension field (Figure 4a).

4.2.2 GSW specimen

Development of the diagonal tension field action through wave-type deformations was observed when the glass fibre infill plate specimen (GSW) was loaded to 3.5 mm displacement and recovered up to 5 mm displacement cycle. Small cracks in the adhesive layer were noticed at 15 mm displacement. No delamination or debonding of the GFRP was visually observed till 20 mm displacement. Between 20 and 25 mm displacement, the GSW specimen experienced delamination in the top corners and at one bottom corners of the infill plate. With the increase of the displacement, further delamination and cracks developed in the direction of the tension field (Figure 4b). The GSW reached ultimate load capacity of 359 kN at 30 mm displacement.



Figure 4. Comparison of damages at 25 mm displacement a) CSW specimen and b) GSW specimen.

4.3 Behaviour of shear walls with hybrid infill plates

4.3.1 HCSW specimens

The development of specimen with hybrid steel/CFRP infill plate went through two stages. The first specimen was constructed with an infill plate attached to the fish plates via simple bolted connection. This specimen failed at early stages of loading mainly due to FRP delamination starting at 5 mm displacement and sliding of the infill plate, which was noticed from 10 mm displacement. Delamination reached 38% of the infill plate area at 30 mm displacement. As a result the design of the HCSW specimen was modified. In the improved design an adhesive layer was applied between the hybrid infill plate and fish plates around the bolted connection with the aim of reducing and delaying sliding of the infill plate. In addition, an adhesive film was applied to improve the bonding between steel plate and FRP layers aiming to reduce delamination.

The improved HCSW specimen showed significantly reduced damage at early stages of loading. The delamination started at 10 mm displacement in contrast to 5 mm previously observed. First signs of sliding of the infill plate at the connection appeared at 15 mm rather than the 10 mm displacement observed in the original design. At 25 mm displacement more significant damages appeared in shape of tearing of the infill plate in a diagonal direction close to the top corners with length of the crack about 50 mm at each of the corners. Soon after that, full length delamination between FRP and steel layers of the infill plate in the area of diagonal tension field developed (Figure 5a). Meanwhile the deformation at the connection with fish plates continued until elongated bolt holes became visible at 30 mm displacement (Figure 5b). The maximum force of 308 kN was achieved at 15 mm displacement.

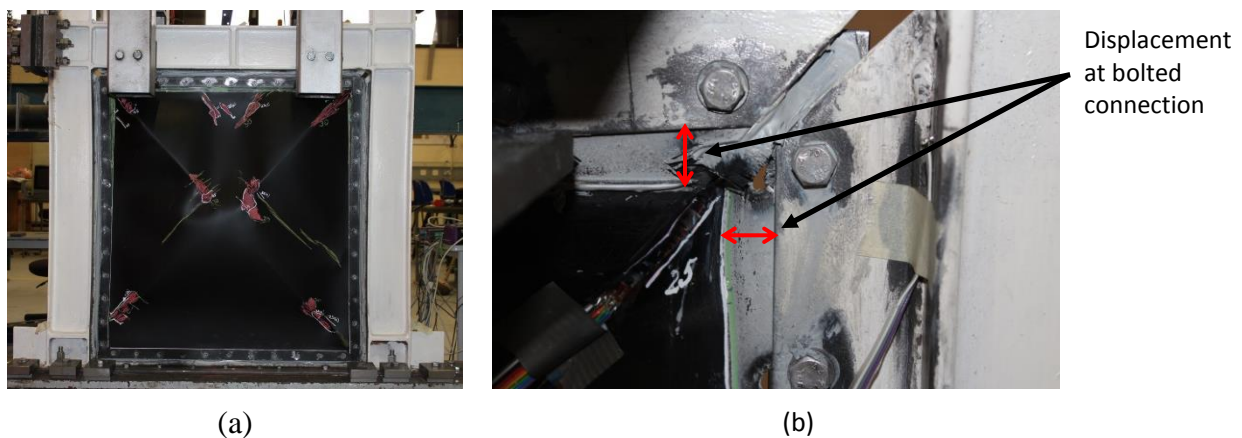


Figure 5. The HCSW specimen at 30 mm displacement loading a) delamination b) failure at the connections.

4.3.2 HGSW specimen

The specimen with hybrid steel/GFRP infill plate (HGSW) obtained visible deformations in diagonal direction due to the tension field at 1.2 mm displacement was noticed. Significant residual deformations appeared at 5 mm displacement, followed by delamination between steel and GFRP at the top corners of the infill plate at 10 mm displacement. At 30 mm displacement diagonal tearing of the GFRP in top corner of the infill plate appeared and the elongation of the bolt holes at the same areas became visible. The HGSW achieved ultimate load capacity of 330 kN at 20 mm displacement. The specimen was tested up to the 30 mm displacement level (Figure 6).

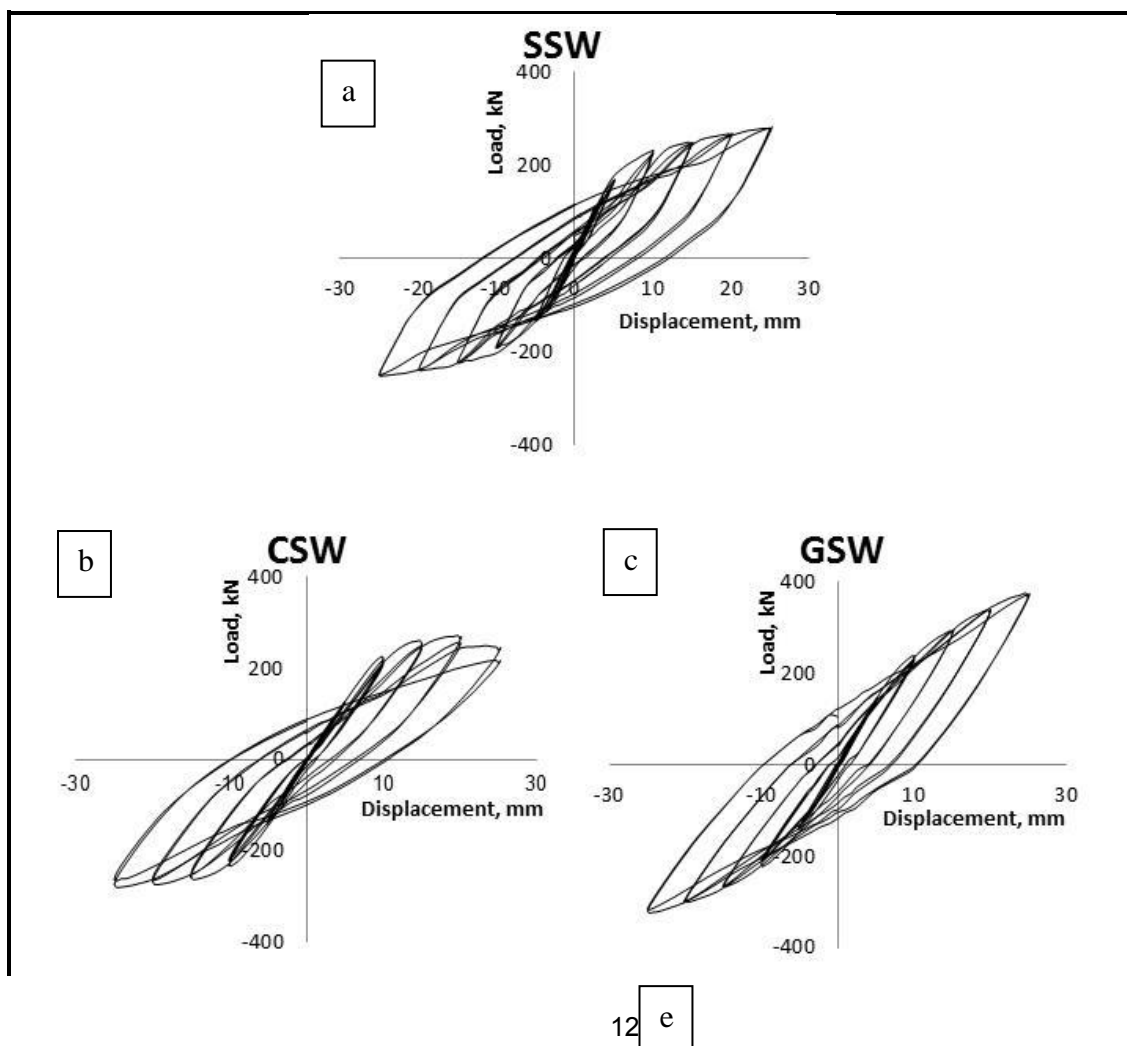


Figure 6. HGSW specimen at 30 mm displacement loading.

5. ANALYSIS OF EXPERIMENTAL RESULTS

The CSW specimen was tested up to the displacement of 25 mm, whereas hybrid carbon (HCSW) and hybrid glass specimen (HGSW) were tested up to 30 mm; steel SW (SSW) and glass GSW specimens up to 35 mm displacement. The tests were terminated when the load could not increase further.

Hysteresis loops for displacements up to 25 mm for all specimens are shown in Figure 7 (a-e).



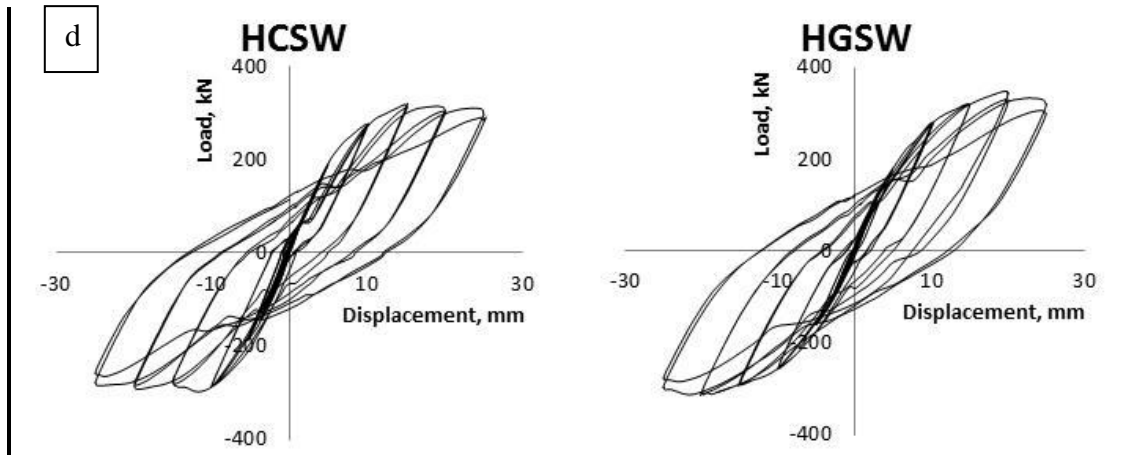


Figure 7. Hysteresis curves for a) SSW b) CSW c) GSW d) HCSW e) HGSW shear wall specimens.

5.1 Normalisation of results

For high-rise buildings, the weight of the structure is a crucial factor in the structural design due to the heavy vertical loading and increased mass and corresponding inertia forces. Table 4 shows the total weight of the shear wall systems (i.e. infill plate and the frame) for different specimens. Due to the low weight of the infill plate compared to the total weight of the shear wall system, the differences between experimental and normalised results were relatively small. As not more than 2% deviation from SSW values was observed, analysis of the data in the paper is based on the experimental data.

Table 4. Weight of the specimen and their factors.

	Weight, kg	Normalisation factor
SSW	77.08	1.00
HCSW	78.53	1.02
HGSW	78.95	1.02
CSW	75.24	0.98
GSW	76.26	0.99

5.2 Comparison of average load values

From the hysteresis loops shown in Figure 7 (a-e), load-displacement curves were estimated by taking the average of the extreme loads for each of the specimens over the cycles at the same amplitude. To estimate the contribution of the infill plate to the capacity of the shear wall specimen, average load results of steel frame only with the same dimensions and made of the same section tested by Maleki, 2012 [23] are added to the Figure 8.

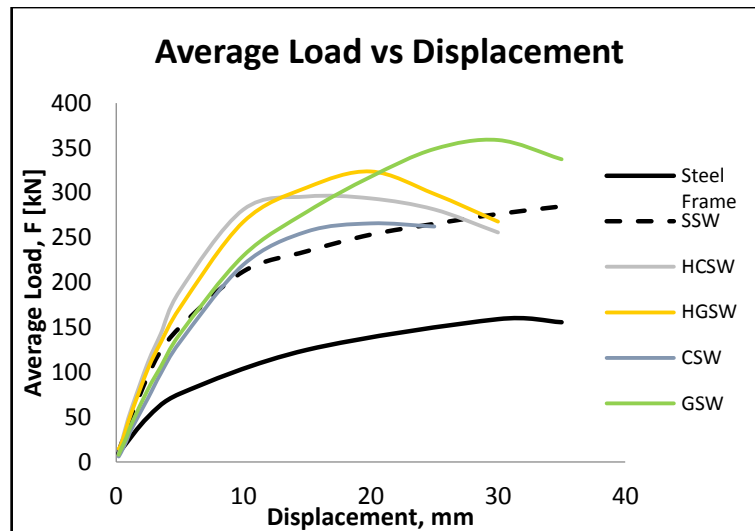


Figure 8. Variation of average load-displacement for five FRP, hybrid and SSW (control) shear wall specimens.

Due to significant contribution of the infill plate, average load results for SSW, pure FRP and hybrid shear walls specimens are significantly higher at displacements larger than 5 mm. Average load of steel frame is approximately 40% lower at 20 mm displacement in comparison to SSW specimen.

For shear wall systems with pure GFRP (GSW) and pure CFRP (CSW) infill plates, the initial load values at the same levels of displacement are lower than the control specimen SSW. This was expected as a result of the lower Young's modulus for FRP. The GSW ultimate load capacity of 359 kN was 35% higher than the CSW ultimate capacity of 266 kN and highest among all the specimens. GSW also showed the highest ductility to reach to maximum load capacity.

For the CSW specimen the main mode of the failure was a sudden and rapid development of delamination between FRP layers and intensive cracking within the CFRP fabric resulting in a relatively brittle failure of the infill plate. In contrast, GSW had a more gradual failure pattern. For GSW delamination was visible only after 20 mm displacement, and was concentrated in the corners along diagonal tension field action.

The load carrying capacities for HCSW and HGSW hybrid specimens are higher at all amplitudes up to 30 mm displacements with respect to control SSW specimen. At 15 mm displacement, the HCSW specimen reaches its ultimate capacity of 308 kN, and at this level of displacement HGSW has similar load value. Between 15 mm and 30 mm displacements, the HGSW specimen showed higher load capacity than the HCSW specimen. The HGSW achieved ultimate load capacity of 330 kN at 20 mm displacement. At 30 mm displacement, a significant destruction of the connection between the infill plate and the fish plates for both specimens occurred and the tests were terminated. As CFRP material is stiffer than GFRP, for the HCSW specimen it is a cause of the

earlier failure as greater level of displacement at the connections between the infill plate and the frame, higher extent of development of delamination and as a result – a lower ultimate load capacity.

For initial stages of loading, hybrid specimens have higher stiffness as they are made with steel plate of the same thickness as SSW specimen but additional layers of FRP were added. Pure FRP specimens have lower stiffness than SSW specimen due to lower Young's modulus of the FRP in comparison to steel.

5.3 Comparison of stiffness values

For the initial loading, all shear wall systems predominantly behave in a linear elastic manner. For control SSW specimen initial stiffness was 37 kN/mm. The hybrid specimens have the highest initial stiffness values. Their stiffness values are between 38 kN/mm and 44 kN/mm. The added layer of CFRP and GFRP to the steel plate contributed to the increase in stiffness. Both GSW and CSW specimens have lower initial stiffness than the control SSW due to lower values of Young's modulus. Their initial stiffness is between 29 kN/mm and 32 kN/mm.

The stiffness at peak load, K_p , for all specimens was found from the slope of the “unloading” curve of the hysteresis curve at the beginning of reversing the displacement (see Figure 9).

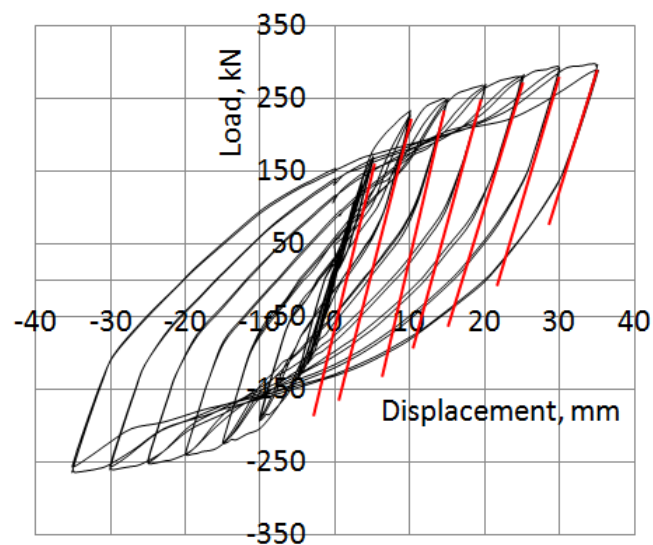


Figure 9. Lines showing variations of stiffness at peak load for SSW specimen.

The degradation of stiffness values at peak load for all specimens during cyclic loading are shown in Figure 10. The HGSW has the highest initial stiffness and CSW the lowest. Although CFRP plates have higher Young's modulus, their stiffness values at the beginning of tested interval of displacements are lower because of influence of slightly lower thickness of CSW infill plates in comparison to GSW infill plates. At larger displacement values, the differences in stiffness values

between CSW and GSW samples increase due to early delamination, cracking and tearing of CSW infill plate.

During cyclic loading the rate of stiffness degradation for SSW, HCSW and HGSW are almost the same. Although GSW has initially a lower stiffness at 30 kN/mm, but the rate of stiffness degradation during cyclic loading in comparison with other specimens is very small and at 25 mm cyclic loading its stiffness is the same as other specimens except CSW which lost nearly half of its stiffness at 25 mm cyclic loading.

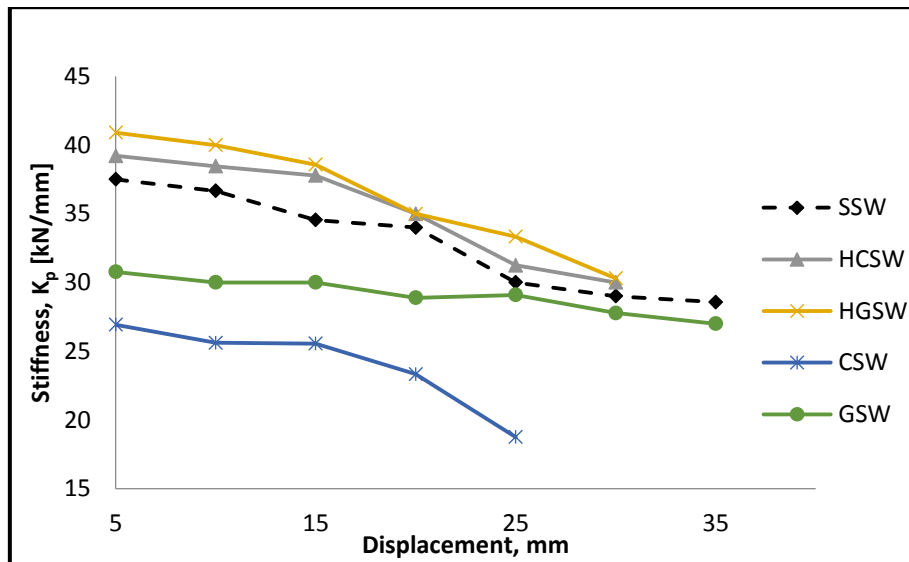


Figure 10. Stiffness values at peak loads for all specimens.

The dynamic stiffness (K_D) for specimens is calculated by measuring the slope between extreme pull and push points at the first cycle of loading at each level of displacement (Figure 11). The evolution of the dynamic stiffness during cyclic loading for all specimens is demonstrated in Figure 12. HCSW had the highest initial dynamic stiffness whilst SSW and GSW had the lowest one. Up to 20 mm displacement, dynamic stiffness for hybrid specimens HCSW and HGSW is higher in comparison with other specimens. The dynamic stiffness for both hybrid specimen continuously decreasing through all loading cycles and at 30 mm displacement they reach approximately to the same dynamic stiffness of SSW due to debonding of FRP laminates from steel infill plate.

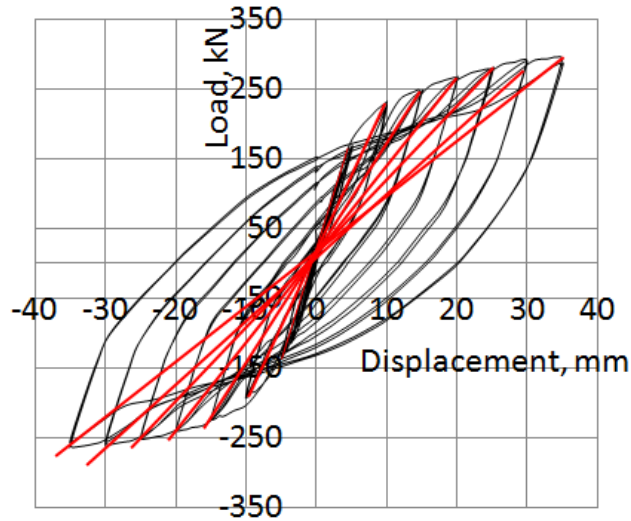


Figure 11. Lines showing history of dynamic stiffness for SSW specimen.

It is noticeable that initially the rate of degradation of K_D for all specimens is nearly the same but after 20 mm displacement GSW attains the lowest degradation in dynamic stiffness. This low degradation rate resulted in the GSW specimen having the highest values of K_D between all specimens above 25 mm displacement.

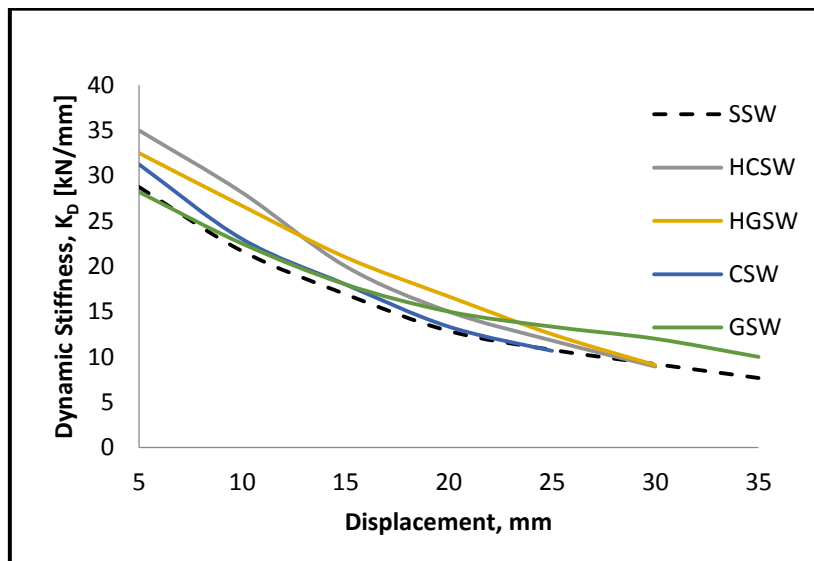


Figure 12. Evolution of dynamic stiffness (K_D) during cyclic loading for all specimens.

5.4 Energy absorption during individual cycle

The variations of the energy absorption during the individual cycles (EIC) at the same level of displacement are shown in Figure 13. The absorbed energy is highest during the first cycle for any applied displacement amplitude and then decreases during the second and the third cycles at the same amplitude for all specimens.

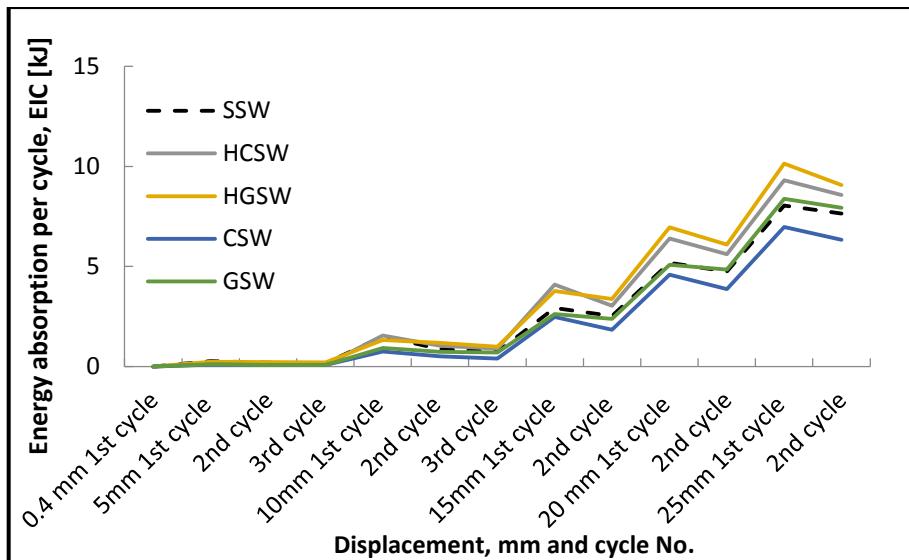


Figure 13. Energy absorption for individual cycles (EIC).

For the SSW, HGSW and GSW specimens the increase in the load is the cause of the gradual increase in the EIC difference between the first and the last cycles at the specific level of loading. For the CSW and HCSW such a tendency is not obvious probably due to the relative brittle failure of the CFRP layers at relatively early stages of loading.

5.5 Energy absorption at any specific level of displacement

According to ATC-24 protocol up to 15 mm displacement three cycles were applied, at 15 mm displacement and above, two cycles were applied. The energy absorption at any specific level of displacement (ESD) was calculated from the sum of the areas of hysteresis load-displacement in all cycles at each level of displacement. Figure 14 shows the energy absorbed by specimens for the tested intervals.

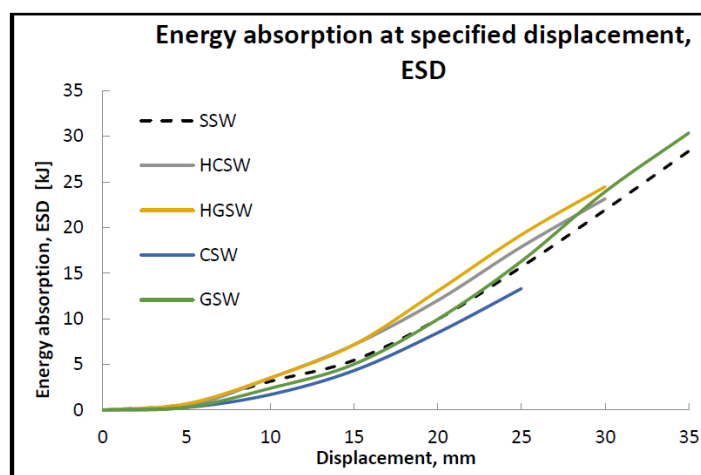


Figure 14. Variation of energy absorption at specified displacement (ESD) for all specimens.

The hybrid specimens HCSW and HGSW have the highest energy absorption in comparison with all the other specimens up to 28 mm displacement; above this level GSW develops higher ESD values. The energy absorption value of HGSW is higher than HCSW specimen for levels of displacement above 17 mm reaching the difference of about 1 kJ at 20 mm and 1.3 kJ at 25 mm, respectively. This is due to the higher deformability of GFRP which delayed the beginning of the delamination process. Hybrid specimens are characterized with significant increase of ESD in comparison with SSW, more clearly visible after 15 mm displacement.

Similarly, for pure FRP specimens, the sample with the GFRP infill plate (GSW) has better behaviour and higher values of ESD than the specimen constructed with pure CFRP infill plate (CSW). The values of energy absorption for the GSW specimen were close to the values of SSW control specimen up to 25 mm displacement. The differences between SSW specimen and GSW started to increase from 25 mm displacement and were 2 kJ at 35 mm displacement. At 30 mm displacement, the ESD values of GSW specimen were similar to HGSW specimen. The ESD of the CSW specimen was lower in comparison with other specimen at all levels of loading.

5.6 Cumulative energy absorption

The cumulative energy absorption (CEA) at specific level of loading was calculated by taking the sum of the ESD for all previous amplitudes. The cumulative energy absorptions for all specimens at 15 mm, 20 mm, 25 mm and 30 mm displacement are shown in Figure 15.

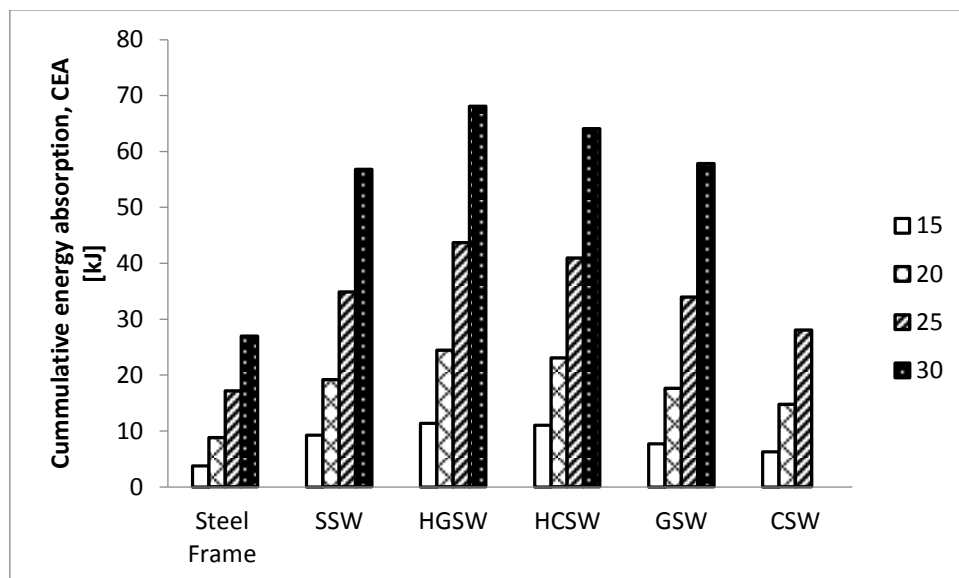


Figure 15. Comparison of cumulative energy absorption (CEA).

Estimated cumulative energy dissipation for steel frame only [23] is approximately 50% lower in comparison to SSW specimen; this difference is even higher in comparison to HCSW and HGSW specimens. For HCSW and HGSW specimens the CEA is higher at all levels of loading in comparison with other specimens. The CEA values for HCSW and HGSW specimens are similar with a

slightly better performance of HGSW. The GSW specimen has slightly lower CEA values than the SSW control specimen for the indicated four levels of loading. The CSW specimen has the lowest CEA in comparison with all the other specimens.

6.0 Conclusions

Ultimate load capacity, deformability, variation in dynamic stiffness and energy absorption of shear wall systems constructed with steel frame and various types of thin infill plates were discussed in this paper. The focus of the study was the comparison between incorporation of pure FRP and hybrid infill plates in shear wall systems.

Specimen with pure GFRP plate (GWS) achieved the highest load capacity, relatively high level of energy absorption within the testing interval, and attained the lowest degradation in dynamic stiffness.

The hybrid carbon (HCSW) and hybrid glass (HGSW) specimens achieved significantly better results in comparison with control SSW specimen for the investigated interval up to approximately 30 mm displacement. The highest energy absorption was achieved by the HGSW specimen when compared with the other specimens. Potential for protection against corrosion for steel infill plates makes hybrid specimens an even more attractive option for future applications.

The investigated innovative shear walls with pure FRP and hybrid thin infill plates offer excellent load capacity, energy absorption, resistant to loss of stiffness and potential for increased durability at significantly reduced weight in comparison with conventional steel shear wall systems. The application of hybrid shear walls for high-rise buildings could be economical and of particular importance potentially reduce the risk of casualties from earthquake events.

Acknowledgement

The authors are grateful for the financial support from Kingston University London and would like to express gratitude to lab technicians in Structural, Composite and Materials Laboratories at Kingston University.

REFERENCES:

- [1] A. Astaneh-Asl, "Steel plate shear walls," *Proceedings, U.S.-Japan Partnership for Advanced Steel Structures, U.S.-Japan Workshop on Seismic Fracture issues in Steel Structures, February 2000, San Francisco.*, 2000.
- [2] T. Roberts, "Seismic resistance of steel plate shear walls," *Engineering Structures*, vol. 17, no. 5, pp. 344-351, 1995.
- [3] M. B. Jadhav and G. R. Patil, "Review on Steel Plate Shear Wall for Tall Buildings," *International*

- Journal of Science and Research*, pp. 973-978, 2012.
- [4] T. Roberts, "Seismic resistance of steel plate shear walls, *Engineering Structures*," vol. 17, no. 5, pp. 344-351, 1995.
 - [5] D. Shen, Q. Yang, Y. Jiao, Z. Cui and J. Zhang, "Experimental investigations on reinforced concrete shear walls strengthened with basalt fiber-reinforced polymers under cyclic load," *Construction and Building Materials*, vol. 136, pp. 217-229, 2017.
 - [6] M. Khazaei Poul, F. Nateghi-Alahi and X. Zhao, "Experimental testing on CFRP strengthened thin steel plates under shear loading," *Thin-Walled Structures*, vol. 109, pp. 217-226, 2016.
 - [7] N. Petkune, T. Donchev, H. Hadavinia, M. Limbachiya and D. Wertheim, "Performance of pristine and retrofitted hybrid steel/fibre reinforced polymer composite shear walls," *Journal of Construction & Building Materials*, vol. 117, pp. 198-208, 2016.
 - [8] ATC-24, "Guidelines for cyclic seismic testing of components of steel structures," Applied Technology Council, California, 1992.
 - [9] L. Thorburn, G. Kulak and C. Montgomery, "Analysis of steel plate shear walls," Dept. of Civil Engineering, University of Alberta, 1983.
 - [10] M. Alinia and M. Dastfan, "Behaviour of thin steel plate shear walls regarding frame members," *Journal of Constructional Steel Research*, vol. 62, no. 7, pp. 730-738, 2006.
 - [11] M. Alinia and M. Dastfan, "Cyclic behaviour, deformability and rigidity of stiffened steel shear panels," *Journal of Constructional Steel Research*, vol. 63, pp. 554-563, 2007.
 - [12] A. Astaneh-Asl., "Seismic behaviour and design of steel shear walls," Structural Steel Educational Council, 2001.
 - [13] A. Rahai and F. Hatami, "Evaluation of composite shear wall behavior under cyclic loadings," *Journal of Constructional Steel Research*, vol. 65, no. 7, pp. 1528-1537, 2009.
 - [14] A. Maleki, T. Donchev, H. Hadavinia and M. Limbachiya, "Numerical modelling and experimental investigation of GFRP-steel sandwich shear walls," in *ICTWS 2011 The 6th International Conference on Thin Walled Structures*, Timisoara, Romania, 2011.
 - [15] A. Maleki, T. Donchev, H. Hadavinia and M. Limbachiya, "Improving the seismic resistance of structure using FRP/steel shear walls," in *Proceedings 6th International Conference CICE 2012.*, Rome, Italy, June 2012.
 - [16] F. Nateghi-Alahi and M. Khazaei-Poul, "Experimental study of steel plate shear walls with the infill plates strengthened by GFRP laminates," *Journal of Construction Steel Research*, vol. 78, pp. 159-172, 2012.
 - [17] A. Rahai and M. Alipour, "Behavior and characteristics of innovative composite plate shear walls," *Procedia Engineering*, vol. 14, pp. 3205-3212, 2011.
 - [18] F. Hatami, A. Ghamari and A. Rahai, "Investigating the properties of steel shear walls reinforced with Carbon Fiber Polymers (CFRP)," *Journal of Construction Steel Research*, vol. 70, pp. 36-42, 2012.
 - [19] N. Petkune, T. Donchev, H. Hadavinia, M. Limbachiya and D. Wertheim, "Investigation of the behaviour of Hybrid Steel and FRP shear walls," in *International Conference CICE 2014, August 2014*, Vancouver, Canada, 2014.
 - [20] N. Petkune, T. Donchev, D. Wertheim, M. Limbachiya and H. Hadavinia, "Application of infrared thermography for assessment of condition of structural element," in *SMAR 2013: Second Conference on Smart Monitoring Assessment and Rehabilitation of Civil Structures. September 2013.*, Istanbul, Turkey, 2013.
 - [21] N. Petkune, T. Donchev, D. Wertheim, H. Hadavinia and M. Limbachiya, "The use of the IRT to assess Steel and FRP hybrid elements," in *SMAR 2015: Third Conference on Smart Monitoring Assessment and Rehabilitation of Civil Structures*, Antalya, Turkey, 2015 .

- [22] ITW Polymers Adhesives, "Devcon Technical Data," 2010. [Online]. Available: http://www.devcon.com/prodfiles/pdfs/fam_tds_180.pdf.
- [23] A. Maleki, "Improving Seismic Behaviour of Steel Plate Shear Walls with and without cut-outs," PhD Thesis, Kingston University London, 2012.